Published in final edited form as:
J Phys Chem B. 2013 October 24; 117(42): . doi:10.1021/jp4020965.

Glassy Dynamics, Cell Mechanics and Endothelial Permeability

Corey Hardin[1], **Kavitha Rajendran**[2], **Greeshma Manomohan**[2], **Dhananjay T. Tambe**[3], **James P. Butler**[3], **Jeffrey J. Fredberg**[3], **Roberta Martinelli**[2], **Christopher V. Carman**[2], and **Ramaswamy Krishnan**[2]

[1]Division of Pulmonary and Critical Care Medicine, Massachusetts General Hospital, Boston, Massachusetts

[2]Center for Vascular Biology Research, Beth Israel Deaconess Medical Center, Harvard Medical School, Boston, Massachusetts

[3]Department of Environmental Health, Harvard School of Public Health, Boston, Massachusetts

Abstract

A key feature of all inflammatory processes is disruption of the vascular endothelial barrier. Such disruption is initiated in part through active contraction of the cytoskeleton of the endothelial cell (EC). Because contractile forces are propagated from cell to cell across a great many cell-cell junctions, this contractile process is strongly cooperative and highly nonlocal. We show here that the characteristic length scale of propagation is modulated by agonists and antagonists that impact permeability of the endothelial barrier. In the presence of agonists including thrombin, histamine, and H_20_2, force correlation length increases, whereas in the presence of antagonists including sphingosine-1-phosphate, hepatocyte growth factor, and the rho kinase inhibitor, Y27632, force correlation length decreases. Intercellular force chains and force clusters are also evident, both of which are reminiscent of soft glassy materials approaching a glass transition.

Keywords

Inflammation; Glass Transition; Cytoskeleton; Monolayer Stress Microscopy; Fourier Transform Traction Microscopy; Cell Mechanics

Introduction

A key feature of inflammatory processes is an increase in the transit of fluid, signaling molecules and white blood cells into the interstitium of injured tissues (*rubor, calor, dolor*). A central regulator of this process is the lining of the luminal surface of vessels – the endothelium. The endothelium is a continuous layer that is only a single-cell thick and challenged with complex and contradictory mechanical requirements. It must maintain its barrier function while remaining compliant and resilient in the face of stretch of the vessel, as occurs routinely with every beat of the heart or inflation of the lung. During inflammatory states, the endothelium must form local gaps to allow the passage of inflammatory cells but

*Corresponding Author: Corey Hardin, Division of Pulmonary and Critical Care Medicine, Massachusetts General Hospital, Bullfinch 148, Boston, MA 02114. chardin@partners.org.

Author Contributions

The manuscript was written through contributions of all authors. Experiments were designed and performed by KR, RK, CVC, RM, CH, and GM. Data analysis was performed by CH. DT developed monolayer stress microscopy and assisted with data analysis. All authors have given approval to the final version of the manuscript.

at the same time maintain its global integrity. Such mechanical properties are conferred to the endothelial monolayer largely by its cytoskeleton.

The cytoskeleton of the endothelial cell (EC) is an active material composed of cross-linked polymers and molecular motors such as myosin, which can contract the fibers. It exists in a continuous state of remodeling[1], metabolizes energy, and is therefore actively displaced away from thermodynamic equilibrium[2]. Its ability to contract, deform, and reorganize are unified by a simple set of empirical principles that are strikingly similar to patterns of behaviors observed in amorphous solids, in particular in soft glasses[3]. Recently, the Wolynes[4] group has reported the results of a model in which the cytoskeleton is treated as an active network of nodes joined by elastic fibers and acted upon by molecular motors. In so doing, they have called attention to the role of the motor proteins in modulating structural rearrangements and thus proximity to an underlying glass transition. The degree to which structural relaxation is promoted or retarded by the motors depends not just on the magnitude of motor activity but also it's interaction with the environment (it's *susceptibility* in the Wolynes model)[4c]. Low susceptibility motors are load resisting – they drive as hard against an uphill potential from the surrounding thermal environment as they do downhill. A susceptible motor, on the other hand, slows down when going uphill. Load resisting motors facilitate structural re-arrangements. In contrast, highly susceptible motors are found to lead to an enhanced attractive interaction between cytoskeletal elements and result in decreased re-arrangements. Much of this work[4a, 4c, 5] has been explicitly aimed at describing the behavior of reconstituted actin/myosin gels and/or isolated cells[6]. The endothelium, however, behaves not as a simple assembly of many individual and independent cells but rather as a coordinated cellular collective. Remarkably, such collective behaviors further deepen the cellular analogy with soft, glassy materials. In a migrating monolayer of endothelial cells, for example, increasing cellular density has been observed to result in a slowing of monolayer structural rearrangement and an increase in the four-point susceptibility similar to that observed in granular materials approaching a jamming transition[7]. Compared to the migrating monolayers studied to date, however, a further complicating feature of the inflamed endothelium is the activation of multiple mechanotransductive signaling pathways[8]. Among these are both barrier protective pathways (which decrease fluid transit across the endothelium) and barrier disruptive pathways (which increase fluid transit across the endothelium) pathways. Ultimately the action of both types is at least partially related to modulation of molecular motors and cytoskeletal contraction[9]. In order to understand how changes in motor activity alter the thermodynamic behavior of cellular monolayers, we present here direct experimental measurements of mechanical changes brought about by barrier-active agents on monolayers of human pulmonary micro-vascular endothelial cells (HLMVEC), and especially their nonlocal and cooperative features.

Each cell in the monolayer exerts forces on both its substrate (e.g., via focal adhesion complexes) and on its neighbors (via vascular endothelium (VE)-cadherin mediated adherens junctions)[9]. Because both VE-cadherin complexes and focal adhesions are bound to the actin cytoskeleton via various linker proteins, these forces ultimately reflect the contractile state of the cytoskeleton and, by inference, it's effective temperature. The effective temperature reflects in part the activity of these molecular motors. Because the molecular motors act on cytoskeletal members, which are joined throughout the monolayer by the cell-cell junctions, the state of each cell is ultimately integrated across the monolayer to determine the global mechanical state. We characterize this global mechanical state using monolayer stress microscopy[7, 10]. Our measurements suggest an unexpected unifying principle: barrier-disruptive pathways are associated with lower effective temperature of the cytoskeleton and greater proximity to a glass transition. Conversely, barrier-protective

pathways are associated with a higher effective temperature of the cytoskeleton and thus a greater distance from an underlying glass transition.

Experimental Methods

Preparation of micropatterned membranes

Repeated patterns of circular islands (diameter = 700 μm, spaced 1.4 mm apart) were fabricated on PDMS membranes as previously described[11].

Preparation of gel substrates

Cell substrates were prepared using polyacrylamide with a physiologically relevant elastic modulus of 1.2 kPa. The protocols for gel preparation, ligation, and handling were similar to published protocols[12]. Briefly, cylindrical gel substrates with a radius of 9 mm and a final thickness of ~100 μm were polymerized upon glass bottom dishes (Mattek Corporation, Ashland, MA). Following polymerization, the gel surface was placed in conformal contact with micropattern membranes and treated with 400 μl of type-1 collagen solution (0.1 mg/ml; Inamed Biomaterials, Fremont, CA).

Cell culture

Human pulmonary microvascular vascular endothelial cells (HLMVEC, Lonza Inc.) were plated as a dense drop (1 million cells/ml) upon the micropatterned surface. Cells preferentially spread within circular micropatterns at an approximately uniform density (Fig. 1b). The spread cells were maintained at 37 °C in humidified air containing 5% CO_2 for two days in EGM-2 cell culture medium (Lonza, Cat#CC-3162) containing 5% Fetal Bovine Serum. Thirty minutes prior to experimentation, the serum-containing media was replaced with a Hank Balanced Salt buffer solution (Life Technologies, Carlsbad, CA) containing 1%Human Serum Albumin.

Measurements – monolayer stress microscopy (MSM)

We recorded spatial maps of fluorescent beads that are embedded within the gel substrate directly underneath the cells. By tracking displacements of the beads and solving the inverse problem of stresses necessary to induce those displacements[13], we quantified the stresses cells exerted on their substrate, referred to here as tractions. From the tractions, we computed intercellular stresses as follows: from Newton's third law, the reversed-sign forces exerted by the cells on the gel are precisely the forces that the gel exerts on the cells. These imposed body forces must be balanced by a build up of stress inside the monolayer (Fig. 1a).

The problem of recovering the intercellular stress tensor within the monolayer is then the problem of determining the two dimensional stress tensor in an elastic layer subject to body forces, which are the imposed reversed-sign tractions. We solve this problem using a finite element analysis as previously described.[7] To complete the intercellular stress recovery, we make mild additional assumptions about material properties, boundary conditions, and, dimensionality. The artifacts associated with these assumptions, both in the recovery of tractions and intercellular stresses, are negligible[10]. MSM therefore yields the local stress tensor everywhere within the monolayer. This 2×2 stress tensor, σ, contains normal stresses (acting perpendicular to adjoining cell membranes) and shear stresses (acting parallel to adjoining cell membranes). These shear stresses are not to be confused with any additional shear stresses associated with fluid flow, which are here assumed to be zero everywhere. We can rotate the local coordinate system to obtain those special orientations in which the shear components vanish thus defining two principal stress components, σ_{max} and σ_{min}. We report intercellular stresses as the average normal stress: $\frac{\sigma_{\max}+\sigma_{\min}}{2}$.

Experimental protocol

Each monolayer was equilibrated on the microscope for 20 minutes. Following equilibration, a pre-treatment baseline measurement was obtained. The monolayer was subsequently treated with one of the following agonists or antagonists: thrombin (agonist, final concentration=0.05 unit/ml); histamine (agonist, final concentration=300 μM); hydrogen peroxide (H_20_2) (agonist, final concentration=1μM); Y-27632 (antagonist, final concentration=0.1μM); Sphingosine-1 phosphate (S1P) (antagonist, final concentration=1μM); hepatocyte growth factor (HGF)(antagonist, final concentration=100ng/ml). Images were recorded for 60 minutes post-treatment. Each of the above agents exerts a time-dependent effect on endothelial monolayer permeability. As we wish to focus on contractile modulation so we ignore later time points (which involve attenuation of agonist/antagonist effects[14]) and calculate stresses only at baseline and the time point corresponding to maximum change in contractile state.

Results and Discussion

The barrier-active compounds studied here are listed in Table I.

We take a highly simplified approach to the complex signaling cascades initiated by each. The three barrier-disruptive agents (thrombin, histamine and hydrogen peroxide) are agonists that have been shown to increase cytoskeletal contraction and, by extension, cell substrate traction forces[15, 20]. The three barrier-protective agents (Y27632, sphingosine-1-phosphate and hepatocyte growth factor) are antagonists that have been shown to relax cytoskeletal contraction[9, 21].

In Fig. 2 we focus on the barrier disruptive/contractile agonists. In accordance with Newton's laws the increase in accumulating cell-substrate tractions must be balanced by an increase in cell-cell forces. Taking the baseline and the time point of maximal change in tractions (data not shown), we then computed the cell-cell forces by means of Monolayer Stress Microscopy[7]. In keeping with the expected balance of forces, we find an increase in intercellular force associated with the action of these contractile agonists. Fig. 2 (a–c) shows the change in the spatial mean (i.e., averaged over the entire monolayer) normal stress. The increase is greatest with thrombin treatment but is also significant in the presence of histamine and H_2O_2.

The local maps of average normal stress with agonist treatment are depicted in Fig. 3 and are striking in at least two respects. The first feature is heterogeneity – the overall impression is of peaks and valleys with closely opposed areas of the monolayer bearing vastly different stresses. Moreover, many peaks represent stresses with a magnitude many times greater than the mean stress. The second striking feature is the longer apparent length scale – i.e. the width of the peaks shown in Fig. 3 spans multiple cell diameters (HLMVEC cells in our preparations having diameters of approximately 20–30 μm).

In Fig. 4, we depict corollary data for the three barrier protective agents (HGF, S1P and Y27632). Compared to the pre-treatment baseline, treatment with HGF yields a decrease in mean local average normal stress of over 15 Pa. Treatment with S1P and Y27632 yield smaller decreases of ~4 Pa and ~8 Pa, respectively. Maps of average local normal stress with treatment are shown in Fig. 4e–f and display the same heterogeneity observed with barrier disruptive treatment.

The extent to which monolayer mechanical behavior is determined by local (i.e. nearest neighbor) or long range forces can be characterized by the spatial autocorrelation function of the stress[7]:

$$C(R)=\frac{1}{N\mathrm{var}(\overline{\sigma})}\sum_{i,j=1}^{N}\sum_{|\vec{r}_i-\vec{r}_j|=R}\delta\overline{\sigma}_i\cdot\delta\overline{\sigma}_j$$

where $\delta\bar{\sigma}_i$ is the local departure of the average normal stress at position $\vec{r}_i$ from its spatial mean $<\bar{\sigma}>$, var($\bar{\sigma}$) is the variance of those departures, and the notation $|\vec{r}_i-\vec{r}_j|=R$ means equality within a uniform bin width of 10 microns. These data are shown in Fig. 5.

At baseline, the correlation function decays only slowly with appreciable correlation (0.4) persisting to 500μm. This represents approximately 20–30 cell diameters. Moreover, the correlation on average increases with barrier disruptive treatment and decreases with protective treatment. In this context it is important to note that barrier disruption does not involve complete separation of neighboring cells. If that were the case, we might expect to see an opposite result with contractile agonists leading to a less correlated state. However, at the concentrations studied here (and in the relevant physiologic range) permeability is increased primarily by the formation of small (nanometer to micrometer[22]) paracellular gaps such that even a highly permeable barrier continues to act as a mechanical whole.

In colloidal materials approaching a glass transition, individual particles form chains of force transmission with a length scale that grows until, at the transition, they may span the entire length of the sample[23]. We sought evidence of such force chains in our endothelial monolayers. To do so, we must modify the calculation of C(R), as the correlation length alone does not specify the geometry of force correlations. Correlated force vectors may align end-to-end, as in a chain, or one next to another, as if marching abreast. We call this later arrangement a force cluster. To assess whether normal stresses are aligned according to either of these configurations, we decomposed the maximum principal stress correlation into chain and cluster contributions,

$$C_{chain}(R)=\frac{1}{N||F||^2}\sum_{i,j=1}^{N}\sum_{|\vec{r}_i-\vec{r}_j|=R}\vec{F}_i\cdot\vec{F}_j\cos^2\theta_{ij}\quad C_{Cluster}(R)=\frac{1}{N||F||^2}\sum_{i,j=1}^{N}\sum_{|\vec{r}_i-\vec{r}_j|=R}\vec{F}_i\cdot\vec{F}_j\sin^2\theta_{ij}$$

Where ||…|| denotes L^2 norm, F_i is the local maximal principal stress considered as a vector quantity (such that the angle between the maximal and minimal principle stress orientations is taken modulo π) and θ_{ij} is the angle between adjacent vector pairs. We present the decomposed correlations for thrombin and HGF in Fig. 6. The total correlation is composed of approximately equal contributions from force chains and force clusters.

Taken together, the data depicted in Fig. 2–4 represent the first comprehensive measurement of intercellular stresses in endothelial monolayers subjected to treatment with barrier-active agents. The traditional view of the process of barrier disruption focuses on local changes in the local balance of forces at the disrupted junction.[9, 24] The notion has been that cell-substrate tractions (acting locally from the cell edge towards the center, thus pulling neighboring cells apart) overwhelming local cell-cell forces (acting to hold neighboring cells together). We take an alternative view suggested by the collective nature of the endothelium. In the intact endothelium, focal adhesions bearing cell-substrate forces and adherens junctions bearing cell-cell forces are both bound to intracellular actin fibers, thus allowing force transmission from cytoskeleton to cytoskeleton throughout the cell layer. Examination of the nature of this force transmission leads to the following new physical picture – barrier disruption is associated with increased intercellular force correlation lengths, non-local

events, and thus an approach *towards* a glass transition. Conversely, barrier protection is associated with decreased intercellular force correlation lengths, and thus movement *away* from a glass transition.

Physical Mechanism

Approach to a glass transition has been suggested to be relevant to diverse collective behaviors ranging from cancer metastasis and wound healing to gastrulation[25]. The data described here add to and deepen this insight by demonstrating a correspondence between endothelial permeability and proximity to a glassy state. The modulation of endothelial permeability has major clinical relevance. Diseases ranging from the acute respiratory distress syndrome[26] and septic shock[27] to autoimmune disorders have as their basis an increased transit across the endothelial layer. How might the action of barrier-active agents modulate the proximity to a glass transition? The proximity[23] of a colloidal system to a glassy state is determined, among other things, by particle stiffness, strength of attractive interaction between the particles, and volume fraction[28]. In that connection, the compounds studied here have pleiotropic effects but can be broadly grouped into their effects on molecular motor proteins and cytoskeletal contraction. Cytoskeletal contraction is the dominant determinant of cell stiffness[29]. In addition to their effects on cytoskeletal contraction some barrier-active compounds can alter the structure of cell-cell junctions by, for example, internalizing VE-cadherins. Within the analogy to colloidal glassy systems, this could be seen as altering the attractive potential between particles.

In much the same way, then, that modulation of cytoskeletal contraction and motor activity are associated with modulation of proximity to an underlying intracellular glass transition[4a], motor protein activity modulates the state of the cellular collective on a continuum from jammed or glassy to un-jammed. This also raises the possibility of novel therapeutic targets for pathologic states defined by increased endothelial permeability – broadly speaking, deceasing motor protein activity should be associated with reversal of increased endothelial permeability.

Future Directions

The compounds studied here represent a small fraction of those known to modulate endothelial permeability. Work in our laboratories is ongoing to classify the activity of additional agents. MSM provides both the full map of cell-substrate tractions (as an intermediate step) and the local intercellular stress tensor everywhere within the monolayer. In principle, these tools allow the full local mechanical characterization of gap formation as well as study of the global events. We focus here on the global mechanical state of the monolayer, but this choice in no way invalidates the importance of local events. A particularly important direction of future investigation involves direct measurement of local forces in the immediate vicinity of a developing paracellular gap. Local force information is provided by MSM, but measurements of endothelial permeability in the literature have, to date, largely involved averaged measures such as electrical resistance and bulk transit of large molecules[30]. In order to correlate with mechanical measurements a local measure of gap formation, such as XPERT[31], is needed. But it remains to be seen whether XPERT can be suitably combined with the simultaneous measurements of intercellular forces.

In conclusion, we demonstrate here that intercellular force transmission in the HLMVEC monolayer is innately collective. We demonstrate further that the characteristic length scale of force transmission responds to barrier active agents in a way that is highly analogous to soft glassy materials approaching a glass transition. Thus, a comprehensive physical understanding of endothelial barrier permeability must include the contribution of cooperative force transmission and glassy dynamics.

Acknowledgments

Funding Sources

NHLBI, Parker B. Francis Fellowship (Krishnan), K25HL111212-01 (Hardin)

NHLBI, HL104006-01 (Carman)

ABBREVIATIONS

MSM	Monolayer Stress Microscopy
FTTC	Fourier Transform Traction Microscopy
HLMVEC	Human Lung Microvascular Endothelial Cell
HGF	Hepatocyte Growth Factor
S1P	Sphingosine-1 Phosphate
MLCK	Myosin Light Chain Kinase

References

1. Seow C, Fredberg JJ. Historical perspective on airway smooth muscle: the saga of a frustrated cell. Journal of Applied Physiology. 2001; 91:938–952. [PubMed: 11457813]
2. (a) Bursac P, Lenormand G, Fabry B, Oliver M, Weitz DA, Visanoff V, Butler JP, Fredberg JJ. Cytoskeletal Remodeling and Slow Dynamics in the Living Cell. Nature Materials. 2005; 4(7):557–561.(b) Bursac P, Fabry B, Trepat X, Lenormand G, Butler JP, Wang N, Fredberg JJ, An S. Cytoskeleton Dynamics: Fluctuations Within the Network. Biochem Biophys Res Commun. 2007; 355(2):324–330. [PubMed: 17303084]
3. (a) Fredberg, J.; Fabry, B. The Cytoskeleton as a Soft Glassy Material. In: Mofrad, M.; Kamm, R., editors. Cytoskeletal Mechanics: Models and Measurements. Cambridge University Press; Cambridge, NY: 2006. p. 50-70.(b) Lenormand G, Fredberg JJ. Deformability, Dynamics and Remodeling of the Cytoskeleton of the Adherant Living Cell. Biorheology. 2006; 43:1–30. [PubMed: 16627924] (c) Fabry B, Maksym GN, Butler JP, Glogauer M, Navajas D, Taback NA, Millet EJ, Fredberg JJ. Time Scale and Other Invariants of Integrative Mechanical Behavior in Living Cells. Physical Review E: Stat Nonlin Soft Matter Phys. 2003; 68:041941–0419418.(d) Zhou E, Trepat X, Park CY, Lenormand G, Oliver MN, Milailovich SM, Hardin CC, Weitz DA, Butler JP, Fredberg JJ. Universal Behavior of the Osmotically Compressed Cell and its Analogy to the Colloidal Glass Transition. Proceedings of the National Academy of Sciences USA. 2009; 106:10632–10637.
4. (a) Shen T, Wolynes PG. Nonequilibrium statistical mechanical models for cytoskeletal assembly: Towards understanding tensegrity in cells. Physical Review E: Stat Nonlin Soft Matter Phys. 2005:72.(b) Wang S, Wolynes PG. Tensegrity and motor-driven effective interactions in a model cytoskeleton. Journal of Chemical Physics. 2012; 136:1451021–14510218.(c) Wang S, Wolynes PG. Microscopic Theory of the Glassy Dynamics of Passive and Active Network Materials. Journal of Chemical Physics. 2013; 138:A521-1-10.
5. Wang S, Wolynes P. On the spontaneous collective motion of active matter. Proceedings of the National Academy of Sciences USA. 2011; 108:15184–15189.
6. (a) Gunst SJ, Fredberg JJ. The first three minutes: smooth muscle contraction, cytoskeletal events, and soft glasses. Journal of Applied Physiology. 2003; 95:413–425. [PubMed: 12794100] (b) Fabry B, Maksym GN, Butler JP, Glogauer M, Navajas D, Fredberg JJ. Scaling the Microrheology of Living Cells. Physical Review Letters. 2001; 87:1481021–1481024.
7. Tambe DT, Hardin CC, Angelini TE, Rajendran K, Park CY, Serra-Picamal X, Zhou EH, Zaman MH, Butler JP, Weitz DA, Fredberg JJ, Trepat X. Collective Cell Guidance by Cooperative Intercellular Forces. Nature Materials. 2011; 10:469–475.

8. Mehta D, Bhattacharya J, Matthay MA, Malik AB. Integrated control of lung fluid balance. American Journal of Physiology - Lung Cellular and Molecular Physiology. 2004; 287:1081–1090.

9. Dudek SM, Garcia JGN. Cytoskeletal regulation of pulmonary vascular permeability. Journal of Applied Physiology. 2001; 91:1487–1500. [PubMed: 11568129]

10. Tambe DT, Croutelle U, Trepat X, Park CY, Kim JH, Millet E, Butler JP, Fredberg JJ. Monolayer Stress Microscopy: Limitations, artifacts, and accuracy of recovered intercellular stresses. PLOS One. 2012 in press.

11. Krishnan RR, Klumpers DD, Park CY, Rajendran K, Trepat X, Bezu Jv, Hinsbergh Vv, Carman CV, Brain JD, Fredberg JJ, Butler JP, Amerongen GPvN. Substrate Stiffening Promotes Endothelial Barrier Disruption Through Enhanced Physical Forces. American Journal of Physiology Cell Physiology. 2011; 300(1):C146–C154. [PubMed: 20861463]

12. (a) Wang N, Ostuni E, Whitesides G, Ingber DE. Micropatterning tractional forces in living cells. Cell Motility and Cytoskeleton. 2002; 52:97–106.(b) Trepat X, Wasserman MR, Angelini TE, Millet E, Weitz DA, Butler JP, Fredberg JJ. Physical Forces During Collective Cell Migration. Nature Physics. 2009; 5:426–430.(c) Krishnan R, Klumpers D, Park CY, Lin Y, Mead JR, jaspers D, Trepat X, Lenormand G, Tambe DT, Smolensky A, Knoll A, Butler J, Fredberg JJ. Reinforcement Versus Fluidization in Cytoskeletal Mechanoresponsiveness. PLOS One. 2009; 4:1–8.

13. (a) Dembo M, Wang Y. Stresses at the cell-to-substrate interface during locomotion of fibroblasts. Biophysical Journal. 1999; 76:2307–2316. [PubMed: 10096925] (b) Butler JP, Tolic-Norrelykke MI, Fabry B, Fredberg JJ. Traction Fields, Moments, and Strain Energy that Cells Exert on their Surroundings. American Journal of Physiology - Cell Physiology. 2002; 282(3):C595–605. [PubMed: 11832345]

14. Vandenbroucke E, Mehta D, Minshall R, Malik AB. Regulation of endothelial junctional permeability. Annals of New York Academy of Sciences. 2008; 1123:134–145.

15. Garcia JGN, Siflinger-Nirnboim A, Bizios R, Vecchio PJD II, JWF, Malik AB. Thrombin-induced increase in albumin permeability across the endothelium. Journal of Cell Physiology. 1986; 128:96–104.

16. Tiruppathi C, Ahmmed GU, Vogel SM, Malik AB. Ca2+ signaling, TRP channels, and endothelial permeability. Microcirculation. 2006; 13(8):693–708. [PubMed: 17085428]

17. Aghajanian A, Wittchen ES, Campbell SL, Burridge K. Direct activation of RhoA by reactive oxygen species requires a redox-sensitive motif. PLoS One. 2009; 4(11):e8045. [PubMed: 19956681]

18. Sun X, Shikata Y, Wang L, Ohmori K, Watanabe N, Wada J, Shikata K, Birukov KG, Makino H, Jacobson JR, Dudek SM, Garcia JG. Enhanced interaction between focal adhesion and adherens junction proteins: involvement in sphingosine 1-phosphate-induced endothelial barrier enhancement. Microvasc Res. 2009; 77(3):304–13. [PubMed: 19323978]

19. Birukova AA, Alekseeva E, Mikaelyan A, Birukov KG. HGF attenuates thrombin-induced endothelial permeability by Tiam1-mediated activation of the Rac pathway and by Tiam1/Rac-dependent inhibition of the Rho pathway. Faseb J. 2007; 21(11):2776–86. [PubMed: 17428964]

20. (a) Budworth RA, Anderson M, Clothier RH, Leach L. Histamine-induced Changes in the Actin Cytoskeleton of the Human Microvascular Endothelial Cell line HMEC-1. Toxicology in Vitro. 1999; 13:789–795. [PubMed: 20654551] (b) Lum H, Malik AB. Regulation of vascular endothelial barrier function. American Journal of Physiology - Lung Cellular and Molecular Physiology. 1994; 267(11):L223–L241.(c) Mehta D, Malik AB. Signaling Mechanisms Regulating Endothelial Permeability. Physiological Reviews. 2006; 86:279–367. [PubMed: 16371600] (d) Yang M, Reich D, Chen CS. Measurement and analysis of traction force dynamics in response to vasoactive agonists. Integrative Biology. 2011; 3(6):663–74. [PubMed: 21445393]

21. (a) Garcia JG, Liu F, Verin AD, Birukova A, Dechert M, Gerthoffer W, Bamberg J, English D. Sphingosine 1-phosphate promotes endothelial cell barrier integrity by edg-dependent cytoskeletal rearrangement. Journal of Clinical Investigation. 2001; 108:689–701. [PubMed: 11544274] (b) Liu F, Schaphorst KL, Verin AD, Jacobs K, Birukova A, Day RM, Bogatcheva N, Bottaro DP, Garcia JGN. Hepacyte growth factor enhances endothelial cell barrier function and cortical cytoskeletal rearrangement: potential role of glycogen synthase kinase-3B. FASEB Journal. 2002; 16:950–962. [PubMed: 12087056] (c) Garcia JGN, Schaphorst K. Regulation of endothelial cell gap formation

and paracellular permeability. Journal of Investigative Medicine. 1995; 43(2):117–26. [PubMed: 7735915]

22. Komarova Y, Malik AB. Regulation of Endothelial Permeability via Paracellular and Transcellular Pathways. Annual Review of Physiology. 2010; 72:463–93.
23. Trappe V, Prasad V, Cipelletti L, Segre PN, Weitz DA. Jamming phase diagram for attractive particles. Nature. 2001; 411:772–5. [PubMed: 11459050]
24. Maruthamuthy V, sabass B, Schwarz U, Gardel ML. Cell-ECM traction force modulates edogenous tension at cell-cell contacts. Proceedings of the National Academy of Sciences USA. 2011; 108:4708–4713.
25. Trepat X, Fredberg JJ. Plithotaxis and emergent dynamics in collective cellular migration. Trends in Cell Biology. 2011; 21(11):638–646. [PubMed: 21784638]
26. Ware L, Mathay M. The Acute Respiratory Distress Syndrome. New England Journal of Medicine. 2000; 342:1334–1349. [PubMed: 10793167]
27. Lee W, Slutsky AS. Sepsis and Endothelial Permeability. New England Journal of Medicine. 2010; 363:689–691. [PubMed: 20818861]
28. Mattsson J, Wyss H, Fernandez-Nieves A, Miyazaki K, Hu Z, Reichman D, Weitz DA. Soft colloids make strong glasses. Nature. 2009; 462(7269):83–86. [PubMed: 19890327]
29. (a) Park CY, Tambe DT, Alencar A, Trepat X, Zhou EH, Millet E, Butler JP, Fredberg JJ. Mapping the Cytoskeletal Prestress. American Journal of Physiology-Cell Physiology. 2010; 298(5):C1245–52. [PubMed: 20164383] (b) Wang N, Tolic-Norrelykke IM, Chen J, Mijailovich SM, Butler JP, Fredberg JJ, Stamenovic D. Cell Prestress. I. Stiffness and Prestress are Closely Associated in Adherent Contractile Cells. American Journal of Physiology - Cell Physiology. 2002; 282(3):C606–616. [PubMed: 11832346]
30. Ochoa CD, Stevens T. Studies on the cell biology of interendothelial cell gaps. American Journal of Physioloogy Lung, Cellular and Molecular Physiology. 2011; 302(3):L275–86.
31. Dubrovsky O, Birukova AA, Birukov KG. Measurement of local permeability at subcellular level in cell models of agonist- and ventilator-induced lung injury. Journal of Laboratory Investigation. 2013; 93:254–263.

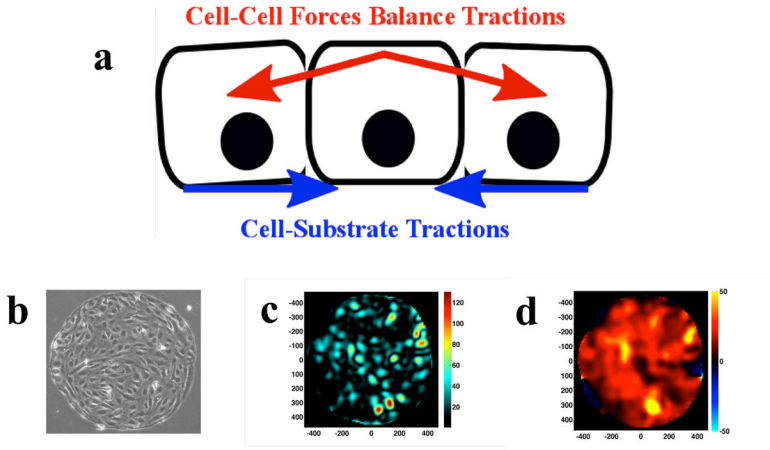

Figure 1. Measurement of Cell Generated Forces

a. The intercellular stress balances the build up of cell-cell substrate tractions. **b**. HLMVEC monolayers are plated on collagen-coated polyacrylamide gels with shear modulus of 1.2 kPa. The gels are prepared with patterned islands of collagen I so that the cells grow to confluence as a 700um island. **c**. Example of traction map (generated with Fourier Transform Traction Microscopy[13b] from which, **d**. the map of intercellular stress can be calculated by MSM.

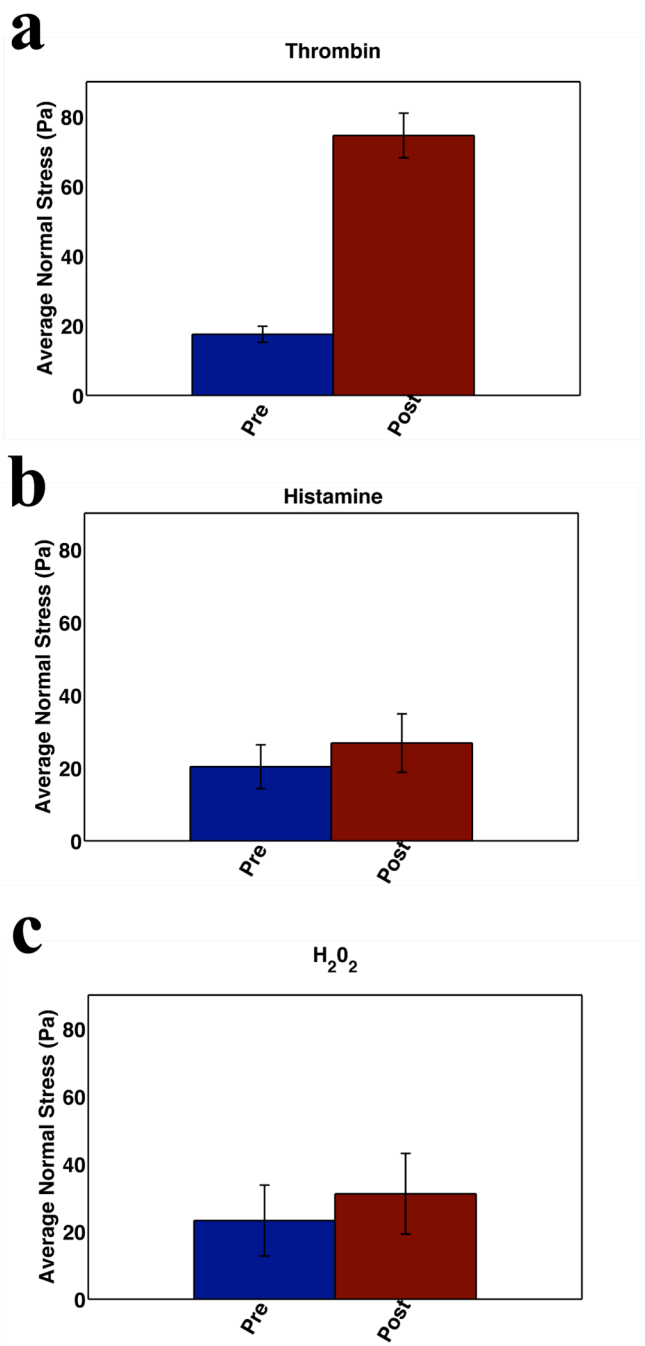

Figure 2. Barrier Disruption

Barrier disruption is associated with an increase in cell-cell forces. Cell-cell forces are measured at baseline and the time point corresponding to maximal increase in contractile moment following agonist treatment. **a** HLMVEC monolayers (N=3) were treated with 0.05 U/ml thrombin and cell-cell forces were measured every 10 minutes for 1 hr. A large increase in average normal stress is demonstrated. **b** HLMVEC (N=2) monolayers treated with 300 μM histamine show increased average normal stress. **c** HLMVEC (N=3) monolayers treated with 10 μm H_20_2 also show a rapid increase in average normal stress.

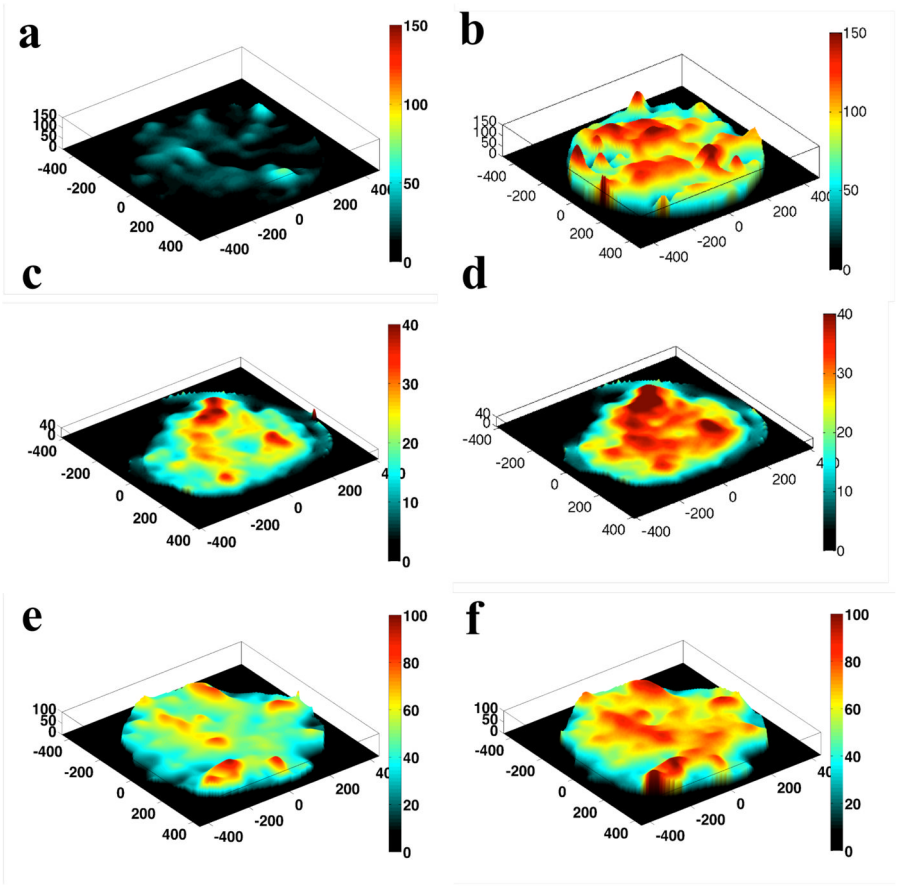

Figure 3. Stress Landscape

There are areas of the monolayer that bear many times the average stress, and neighboring areas of the monolayer can experience drastically different stresses. The ruggedness of the landscape is enhanced with agonist treatment. **a**, baseline HLMVEC monolayer **b**. monolayer after thrombin treatment (0.05 U/ml). Note the larger scale on the z-axis compared to subsequent maps. This is necessary due to the comparatively large stresses that result form thrombin treatment. **c**. baseline monolayer and **d**. monolayer after treatment with 300 μM histamine. **e**. baseline monolayer and **f**. monolayer after treatment with 10 μM H_20_2.

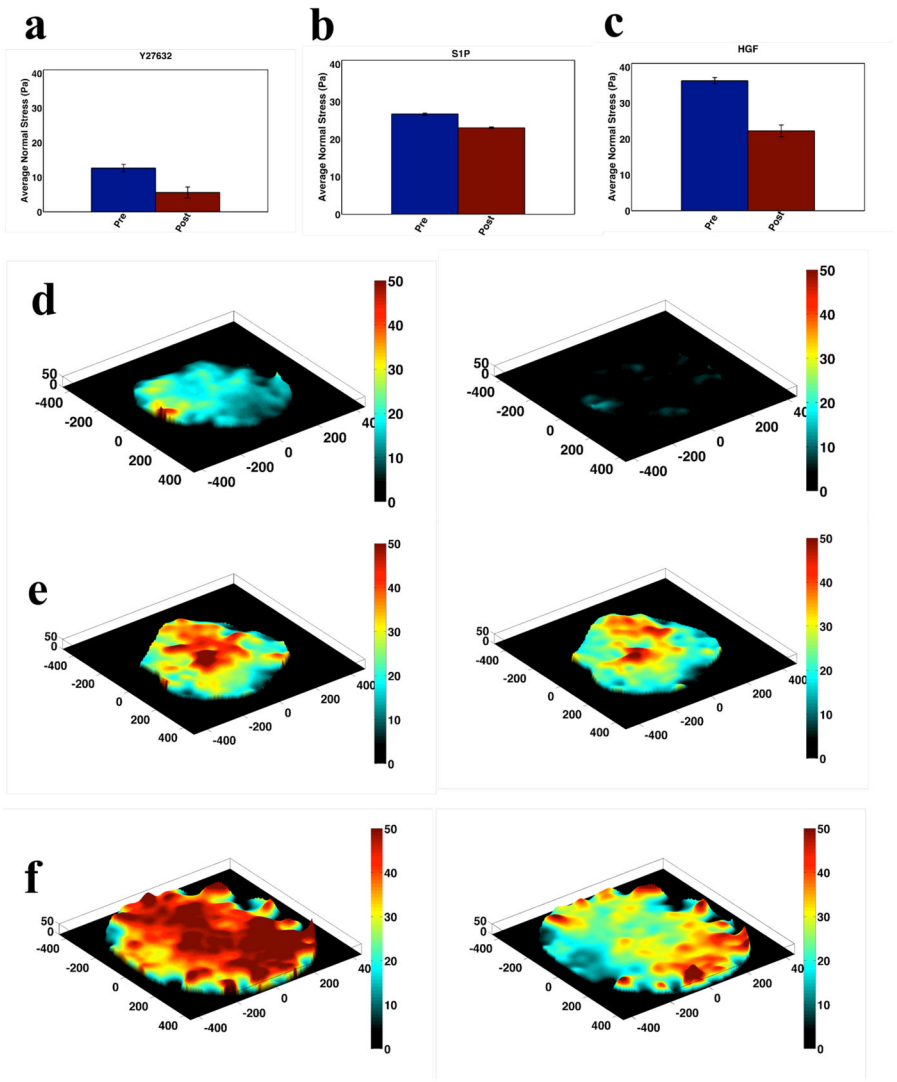

Figure 4. Mechanics of Barrier Protection

Intercellular normal stress for HLMVEC monolayers before and after treatment with barrier protective agents 0.1 μM Y27632 (**a**. N=4), 1 μM S1P (**b**. N=2) and 100 ng/ml HGF (**c**. N=4). In all cases, post-treatment stresses are measured at the time point corresponding to minimal post-treatment contractile moment. Corresponding maps of local average normal stress pre and post treatment are shown for Y27632 (**d**), S1P (**e**) and HGF (**f**).

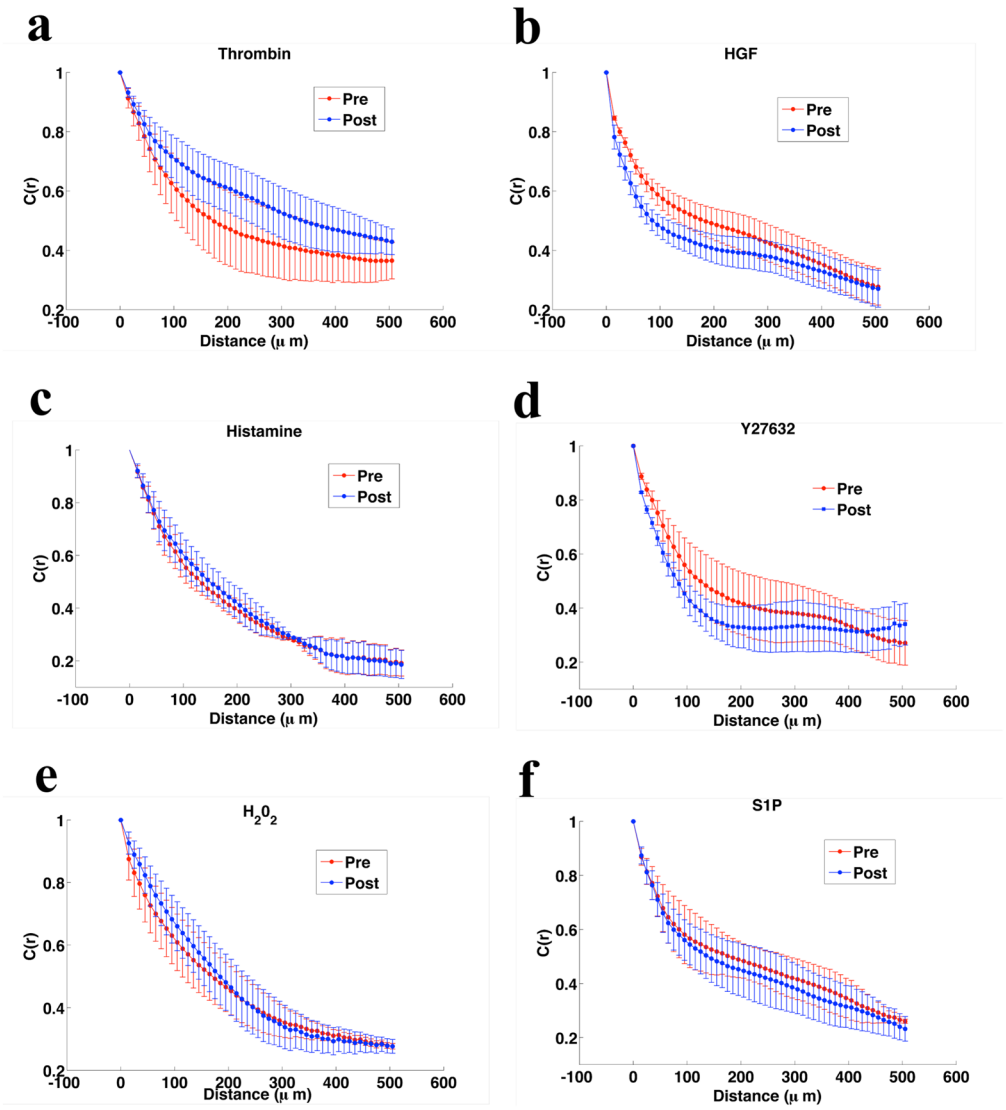

Figure 5. Effect of Barrier Modulation on Force Autocorrelation Length

For the three barrier disrupting compounds and the three barrier protective agents C(r), the spatial autocorrelation function of the average normal stress, is calculated at baseline and at peak effect. The correlation length is increased with barrier disruption (**a**. Thrombin, **c**. Histamine, and **e**. H_20_2) and decreased with barrier protection (**b**. HGF, **d**. S1P, and **f**. Y27632).

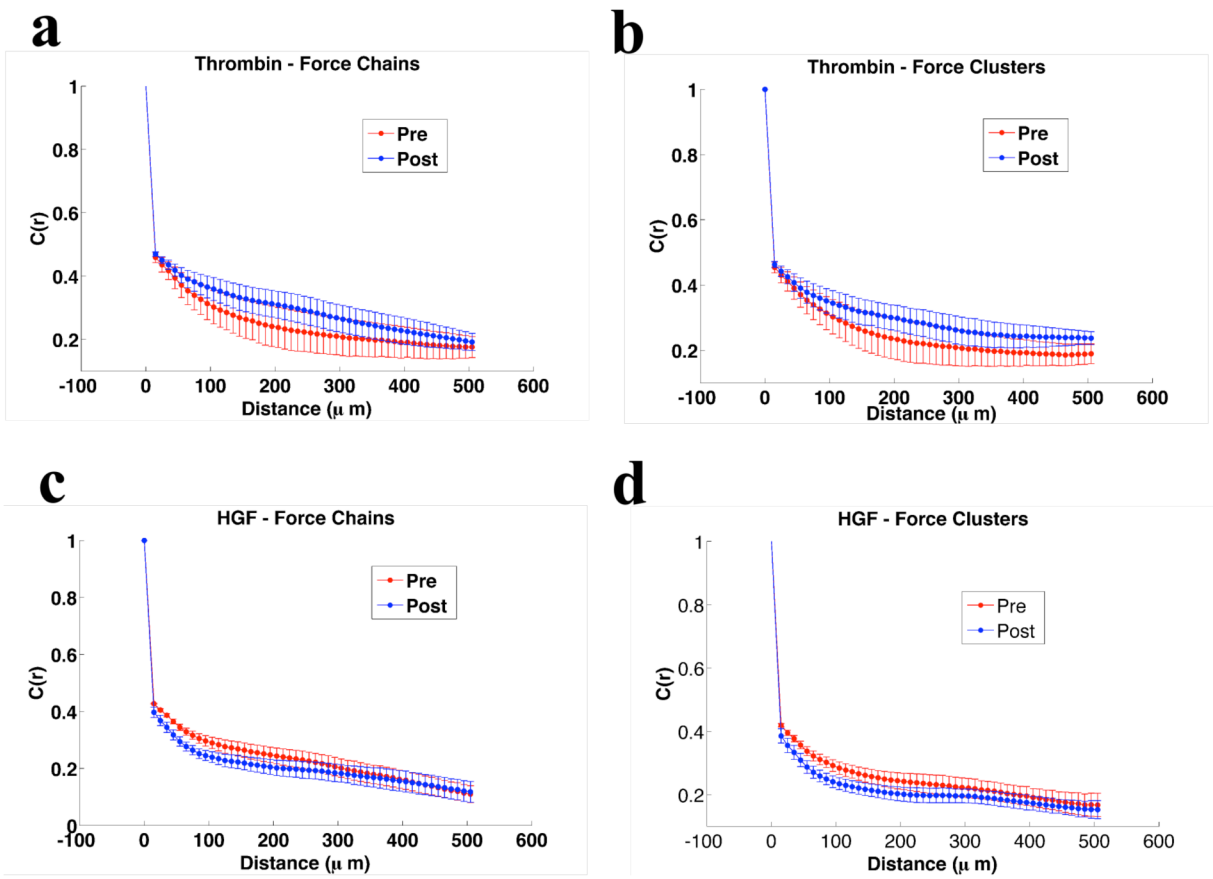

Figure 6. Geometry of Force Correlation

The correlation length alone does not reveal the geometry of emerging force structures. For the examples of thrombin (**a**–**b**) and HGF (**c**–**d**), the increasingly long distance correlations are seen to be roughly evenly divided between force chains (**a.** and **c.**) and force clusters (**b.** and **d.**).

Table 1

Barrier Active Compounds and their Mechanism of Action

Compound	Effect on Permeability	Mechanism of Action
Thrombin[15]	Increase	Formation of stress fibers to subsequently increase cell contraction
Histamine[16]	Increase	Increased intracellular Ca^{++} and Myosin Light Chain Kinase(MLCK) induced contraction
Hydrogen Peroxide (H_20_2)[17]	Increase	RhoA activation, MLCK induced contraction
Y27632[8]	Decrease	Cytoskeletal relaxation via Rho inhibition
Sphingosine-1phosphate (S1P)[18]	Decrease	Cadherin reorganization and cytoskeletal relaxation.
Hepatocyte Growth Factor (HGF)[19]	Decrease	Rac/Rho mediated cytoskeletal relaxation